Characteristics of regenerated nanocellulosic fibers from cellulose dissolution in aqueous solutions for wood fiber/polypropylene composites

Sangyeob Lee[1], Hui Pan[2], Chung Y Hse[3], Alfred R Gunasekaran[4] and Todd F Shupe[5]

Abstract

The effects of aqueous solutions were evaluated on the properties of regenerated cellulosic nanofibers prepared from pure cellulose fibers in various formulations of aqueous solutions. Thermoplastic composites were prepared with reinforcement of the regenerated cellulosic nanofibers. The regenerated cellulosic fibers from cellulosic woody biomass were obtained from dissolved cellulose solutions by coagulating with sulfuric acid and water for phase separation. The properties of the regenerated cellulosic fibers were characterized using Fourier-transform infrared spectroscopy (FTIR), wide angle X-ray diffraction (WAXRD), thermogravimetric analysis (TGA), field emission scanning electron microscopy, and tensile testing. The TGA, WAXRD, and FTIR spectra indicated that the regenerated nanofibers possessed cellulosic crystal type II. The micrographs of regenerated cellulosic fibers showed a dense composite structure and lower crystallinity than controlled fibers. The tensile strength of regenerated cellulosic fiber-reinforced polymer composites reached 30 MPa, which was 70% higher than the

[1] Mississippi Pacific Resins Inc., Starkville, MS, USA
[2] Calhoun Research Station, Louisiana State University Agricultural Center, Calhoun, LA, USA
[3] Southern Research Station, USDA Forest Service, Pineville, Louisiana, USA
[4] The Institute for Micromanufacturing, Louisiana Tech University, Ruston, Louisiana, USA
[5] School of Renewable Natural Resources, Louisiana State University AgCenter, Baton Rouge, LA, USA

Corresponding author:
Sangyeob Lee, Mississippi Pacific Resins Inc., P. O. Box 412, Starkville, MS 39760, USA.
Email: lsy6709.mpresin@gmail.com

control fiber-reinforced composites. The composites prepared from regenerated fibers with sodium hydroxide (NaOH)/urea and NaOH/urea/thiourea aqueous solutions provided the best results. This work also provides a potential promising method to efficiently obtain nanocellulosic fibers as reinforcement materials in bio-based nanocomposites.

Keywords
Aqueous solutions, regenerated cellulose, biocomposites, nanofibers

Introduction

Natural nanofibers have received increased attention because of their properties and performance for reinforced composite materials. Due to extensive applications with biodegradable, renewable, low-cost, lightweight, and abundant resources, cellulosic nanofibers have been generated through many different processes. The processes used were complicated and involved multitreatment stages.[1–3] The processes were also hindered by high production cost, high energy consumption, increased material loss, and environmental issues. Recently, a repeating freezing/thawing process in aqueous solutions associated with swelling agents has been introduced to regenerate cellulosic fibers, films, and membranes.[4–7]

Cellulose is comprised of repeating units of glucose pyranoses linked by β-1-O-4 glycosidic bonds and a main skeletal component (40–45%). Cellulose is also insoluble in water because of the strong hydrogen bonding between the cellulose chains.[8,9] In order to dissolute cellulose, strong acids and alkali solutions have been used with catalysts, depending on material conditions and applications.[3,10–12] The treatment altered surface characteristics, such as hydrophobicity, morphology, surface roughness, thermal characteristics, and crystal types. The repeated freezing/thawing process in aqueous solutions provided increased dissolution of cellulosic materials. Additional cellulose dissolution was reported using urea and thiourea as a swelling media.[2,9,13] The aqueous reagents need to interact at the hydroxyl group interface and penetrate the structure; therefore, swelling of the structure is an important factor in dissolving cellulose.

Cellulose also consists of crystalline and amorphous regions. A series of wide angle x-ray diffraction (WAXRD) studies have shown that the degree of crystallinity and cellulose type can be changed by chemical treatments. The degree of crystallinity decreases in the order of cotton, wood pulp, mercerized cellulose, and regenerated cellulose.[8] The XRD patterns indicated cellulose type I was transferred to cellulose type II due to the strong alkali treatment to regenerate cellulose with decreased crystallite sizes.

Many volatile, toxic, and relatively high-cost processes were introduced to dissolve cellulose using derivative and nonderivative solvents.[7,14,15] Among the solvents, N-methyl-morpholine-N-oxide/water system and cadmium chloride ($CdCl_2 \cdot 2.5H_2O$), were reported to be the most powerful cellulose solvent with excellent property enhancement for the regenerated cellulosic materials.[14,16–18] However, the process produced considerable amounts of residues and by-products as well as reductions in glucose units.

Table 1. Treatment conditions for cellulose fibers at a fiber to liquid ratio of 1:30.

Treatment ID	Treatment temperature (°C)	Liquid ratios NaOH/Urea/Thiourea/H$_2$O	Note
T1	−5	8.5/0/0/91.5	
T2	−8	8.5/0/0/91.5	
T3	−12	8.5/0/0/91.5	
T4	−12	8.5/0/0/91.5	Heat treatment at 60°C
T5	−12	6.9/12/0/81	
T6	−12	8.1/8.1/6.5/77.4	

NaOH: sodium hydroxide; H$_2$O: water.

Furthermore, the effective solvent recovery system is yet to be developed. It is not suitable to regenerate nanocellulosic materials from the aqueous solution. The other effective dissolving processes developed recently are sodium hydroxide (NaOH)/urea, NaOH/thiourea, and NaOH/urea/thiourea aqueous solutions.[9–13] The dissolving process associated with swelling agents provided a simplified technology to directly dissolve cellulose quickly with relatively lower cost, lower toxicity, and yield regenerated fibers with enhanced strength properties as reinforced materials. However, the process was developed on utilizing cotton fibers to produce films or membranes and limited studies subjected for reinforcement materials. The objective of this study was to generate nanocellulosic fibers as reinforcement materials from wood-based cellulosic biomass without weight loss during the treatment process. This study is also conducted to develop simple treatment steps with relatively low chemical consumption to increase economic viability.

Experimental

Materials. Whatman grade no. 1 filter paper (99.9% pure cellulose with less than 0.06% ash content) was used as raw cellulose fibers, which were defiberated using a lab scale disintegrator to minimize structural damages to the natural fibers. The filter paper and chemicals used for this study were of analytical grade and were purchased from Fisher Scientific Co. LLC (Pittsburgh, PA, USA). Commercially supplied polypropylene (PP; EXXON PP-7292W, Houston, TX, USA) was used as a matrix material. The mixtures were mechanically compounded in a laboratory miniature molder (LMM-4-120, Qualitest, Buffalo, NY, USA). A compounding mixing ratio consisted of 20% regenerated cellulosic fibers and 80% PP.

Fiber preparation

The filter paper sheets were defiberated, dewatered, and dried at 80 ± 0.5°C for 24 hrs before being used. Cellulosic fibers of 10 g were weighed and pretreated in 17.5 wt% NaOH for 24 hrs under ambient temperature and 400 r min^{-1} to obtain pure cellulose fibers. The pretreated fibers had 12 wt% weight loss. The fiber to liquid ratio was 1:30 to obtain free condition for fibers. The pretreated fibers were filtered and dried in a freeze

dryer for 24 h. Table 1 shows the controlled treatment temperatures and formulations for the aqueous solution used to prepare cellulose solutions.

A designed formulation of NaOH, urea, thiourea, and distilled water were added into a 50-mL flask and stirred under ambient temperature until the added chemicals were completely dissolved. Freeze-dried cellulose fibers (1 g) were dispersed into an aqueous solution mixture and were stirred together at a stirring speed of 300 r min^{-1} for 3 h. The resulting cellulose slurry was held at low temperatures to be frozen and then thawed with intermittent mixing at $-4°C$ for 2 h. The slurry was transferred to a temperature-controlled refrigerated bath (NESLAB RTE7, ThermoFisher Scientific LLC, Pittsburgh, PA, USA), with target temperatures of -5, -8, and $-12°C$ for 1 h to obtain transparent solutions. Heat treatment was applied during the degassing stages for samples of treatment 4 (T4). The other samples were degassed under ambient temperature with vigorous stirring for 20 min to obtain transparent cellulose solutions at a concentration of 3.3 wt%. The NaOH consistency of the aqueous solution mixture was adjusted to 5 wt% by adding water (H_2O) into a flask-containing cellulose solution. The resulting cellulose mixtures were stored for 48 h in a refrigerator at $4°C$.

The resulting filtered cellulose fibers were cleaned of excessive chemicals with H_2O, and the H_2O was collected for coagulation. The additional H_2O in the aqueous solution and filtering stage acted as a coagulant. Cellulose in the gel was regenerated through the coagulation process to form cellulosic fibers. The collected regenerated fibers were dried in a freeze dryer under vacuum for 24 h. To coagulate, the collected aqueous liquids and cleaned liquids were titrated to adjust the pH to 6.5 with 72 wt% sulfuric acid (H_2SO_4) at $20°C$. The clear solution started to form white nanocrystal drops. The regenerated cellulose was isolated by a phase separation method using a centrifuge (Sorvall Legend T Plus EASYset™, ThermoFisher Scientific LLC, Pittsburgh, PA, USA) at 4000 r min^{-1} for 30 min and dried in a freeze dryer.

Characterization

The dynamic viscosities of the aqueous liquids were determined, according to the Council of Europe,[19] using a size II capillary U-tube viscometer at a temperature of $20 \pm 0.5°C$. The average of the three readings was used to determine the flow time of the liquid to be examined.

The dynamic viscosity (η) was calculated using the following formula:

$$\eta = k\rho t$$

where k ($= 0.1$ mm^2 S^{-2}) is the constant of the viscometer; ρ is density of the liquid; and t is flow time (in seconds) of the liquid to drop from one mark to the other.

Fourier-transform infrared (FTIR) spectra were recorded using a FTIR spectrometer (NEXUS™ 670 FTIR E.S.P.; Thermo Nicolet, ThermoFisher Scientific LLC., Pittsburgh, PA, USA) equipped with "Smart Golden Gate" and midrange (4000–650 cm^{-1}) capabilities. The powder form of regenerated cellulose fibers was vacuum dried for 24 h before the measurement. The test samples were placed under the golden gate fixture and spectra collected under ambient temperature with 40 scan rates. The data acquisition software was OMNIC 5.2.

XRD was carried out with a wide angle x-ray diffractometer (Bruker D8 Discover, Bruker AXS, Germany) with PILOT v2009.3-0 for data acquisition. The powder form of regenerated cellulose fibers were vacuum dried for 8 h and stored in a desiccator before collecting the XRD patterns. The XRD patterns with copper X-unit (CuKα) at 40 kV and 40 mA were recorded in a range of 2θ from 5 to 40°. The degree of crystallinity (X_c) was calculated using the XRD patterns.[20]

The thermogravimetric analysis (TGA) of the regenerated cellulose fibers was carried out on a TGA Q50@Srs (TA Instrument, New Castle, DE, USA) under nitrogen atmosphere at a heating rate of 10°C min^{-1}. The thermal degradation of the fibers was investigated at ranges from 150 to 450°C. Testing from 450 to 650°C was also conducted to monitor the continual char deformation. The thermal changes were expressed as onset temperature (T_{onset}), maximum degradation temperature (T_{peak}), and offset temperature (T_{offset}).

The morphology of the regenerated cellulose fibers from the aqueous cellulose gel was investigated using field emission scanning electron microscopy (FESEM; Hitachi S-4800, Japan) with RE-232C interface. Mounted regenerated fibers were coated with an approximately 6-nm thin gold layer using an ion sputter (Cressington Sputter Coater 208HR equipped with a thickness controller 2.0) to minimize charging during the observation. The morphological characteristics were analyzed using the photomicrographic images to identify the fiber surface conditions. Images were generated at 2 kV and up to 40,000× magnification.

The tensile test samples were compounded with 20% regenerated nanofibers/80% PP using a laboratory miniature injection molder. The reinforced tensile samples were prepared with 20% pure cellulose reinforcement in a 80% PP matrix. The extruded compounds were transferred to a 154 × 154 mm^2 hot press. Test samples were cut to 38 mm in length and 5.7 mm in narrow-neck width, 0.2 mm in thickness, and 22 mm between the two clamps. The tensile strength of the nanofiber-reinforced PP composites was measured on a Instron testing machine (Instron 4465, Instron, Norwood, MA, USA), according to ASTM D638-10[21] at a crosshead speed of 6.5 mm min^{-1}. The reported values are the averages of five samples. Standard deviations were also calculated.

Results and discussion

Figure 1 shows the changes of the regenerated cellulosic fiber fraction associated with the treatment conditions. The regenerated fiber types were retained from the fiberglass filter, filtered aqueous solution, and cleaned weak aqueous solution. Most retained fibers were obtained at the initial water coagulation for 48 hours in the refrigerator. A series of regenerated cellulose fibers were prepared from the cellulose solution by coagulating with 72% H_2SO_4 and H_2O. A total of 70–90% of retained fibers were collected by filtration. The H_2SO_4 coagulation provided additional 8–27% regenerated cellulosic fibers. Coagulation with additional water to make 5 wt% NaOH was less effective to regenerate nanocellulosic fibers from the liquid gel form associated with the swelling agent and temperature treatments. Lower treatment temperatures provided increased cellulose dissolution as well as less coagulation using H_2O to regenerate nanocellulosic fibers. Nanofiber yields from each step of the cellulose regeneration added up to 100%
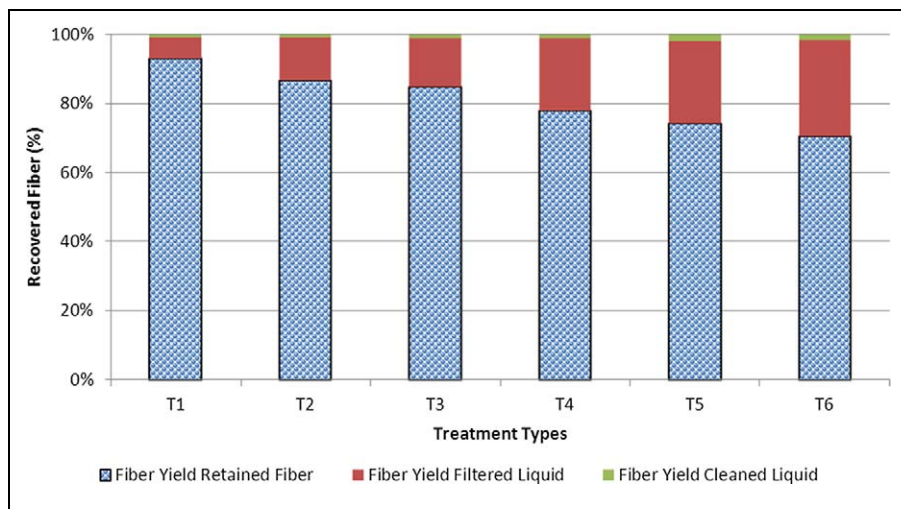
Figure 1. Yields of regenerated cellulosic fibers formed from the filtering stages of cellulosic aqueous solutions.

material recovery from the aqueous liquid gel. The figure also indicated that lower temperature treatment, swelling agent, and additional heat treatment provided increased cellulose dissolution in the aqueous solution.

The viscosities of the dissolved cellulose in 8.1–8.5 wt% NaOH with/without 8 wt% urea aqueous solutions and a desired amount of thiourea that compared the base aqueous solutions and different treatment conditions are shown in Figure 2. This result also indicated that viscosity increased along with treatment temperatures and the presence of swelling agents. The highest viscosity was obtained from the aqueous solution that contained urea and thiourea as swelling agents during the repeated freezing/thawing process. It is interesting to note that the swelling agents provided the best condition to dissolve the cellulosic fibers. The swelling agents penetrated into the intermolecular structure and optimized structural failure of the cellulosic materials.

As shown in Figure 3, the FTIR spectra of all the obtained powder forms of the regenerated cellulosic fibers showed typical bands at 1038 cm^{-1} (the C–O in cellulose), together with those at 1460/1415 cm^{-1} and 885 cm^{-1}. The peak at 896 cm^{-1} is assigned to the deformation of anomeric C1–H or the antisymmetrical out-of-phase ring stretching, which represents crystal type II from regenerated cellulosic fibers. The 1420 and 1068 cm^{-1} peaks, assigned to the symmetric bending of CH$_2$ and C3–O stretching, respectively, also shifted to higher wave numbers because of the interaction between the cellulose chain and aqueous solutions. The band at 2900 cm^{-1} was assigned to asymmetrically stretching vibration of C–H in pyranoid rings. The peaks at 3000–3650 cm^{-1} correspond to stretching vibrations of hydroxyl groups of cellulose noticeably moved to higher wave numbers and became broader and stronger, indicating a strong interaction between exposed hydroxyl groups and aqueous solutions.
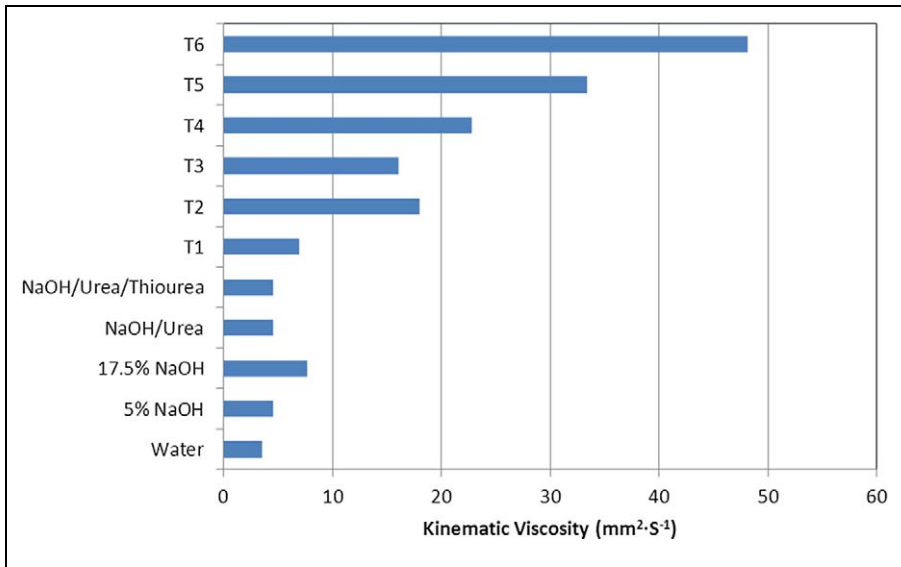
Figure 2. Kinematic viscosities of aqueous solutions at the levels of chemical ratios.

Figure 4 shows the WAXRD patterns of the regenerated cellulosic fiber samples from NaOH-based aqueous solutions through the coagulation process. The diffraction peaks observed at around 14.2°, 15.6°, and 21.9° in 2θ were attributed to natural cellulose. All the other diffraction peaks in WAXRD patterns can be indexed to each crystalline phase with a hexagonal structure. The peaks at 11.5°, 19.1°, and 21.6° for 2θ correspond to the deflection angles of regenerated nanocellulosic fibers. Apart from the diffraction peaks of fibers, there are additional peaks in the pattern indicating that the crystallized cellulose fibers regenerated thermodynamically favored hexagonal structure. The observed rising background centered at 22.08° is as a result of the presence of the amorphous region of cellulose. Chemical treatments altered crystal types of cellulose even in the pretreatment stage. Regardless of the aqueous solution types and treatment temperatures, crystal type was transformed from type I to type II in transition stages. The broad nature of the WAXRD peaks could be attributed to the presence of nano-sized structures. In view of the WAXRD and FTIR results, all the regenerated nanofibers were reformed in crystal formation due to the strong interaction of the exposed hydroxyls and aqueous solutions associated with the swelling agents.

The thermal parameters of the regenerated cellulosic fibers used in TGA are shown in Table 2. The TGA results showed a small weight loss around 100°C corresponding to H_2O desorption. The weight loss around 220 and 321°C indicated the thermal degradation and completed decomposition of regenerated cellulosic fibers coagulated from the aqueous solutions. The TGA revealed about 65–75% weight loss of the cellulose used for the thermal analysis. The peak temperatures at a range of 250–302°C for the regenerated nanofibers are associated with cellulose decomposition as indicated
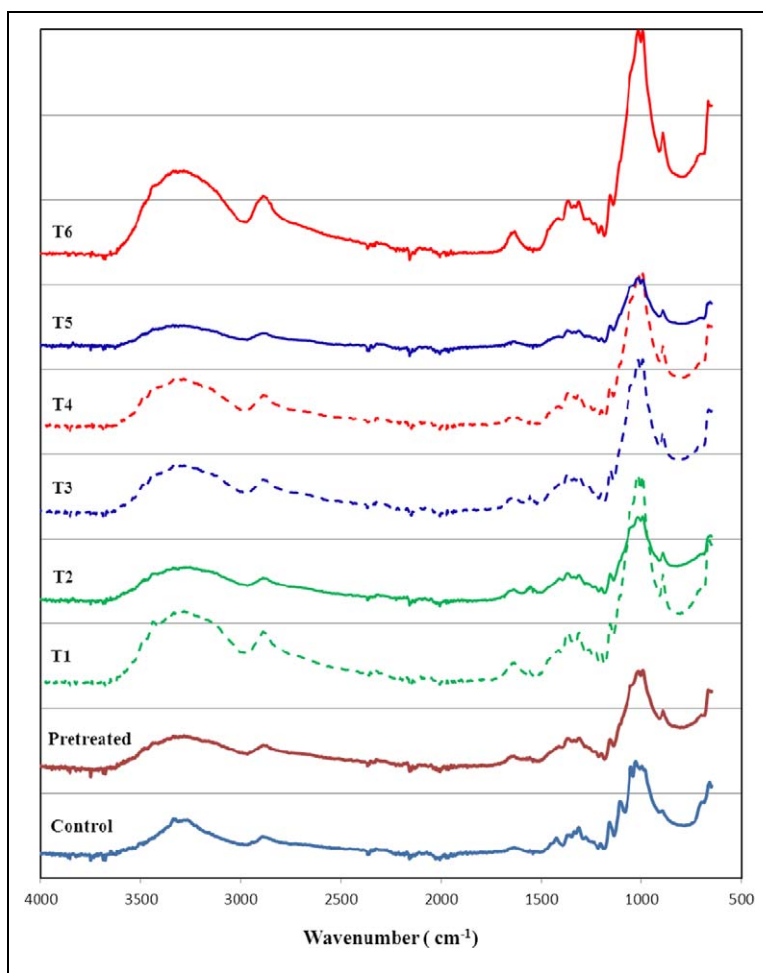
Figure 3. Fourier-transform infrared spectra of the regenerated cellulosic nanofibers prepared by a repeated freezing/thawing process using aqueous solutions at different temperatures.

in the TGA results. The decomposition peaks of the nanofibers shifted to low temperature because of a relatively easy motion of cellulose molecules. The peak decomposition temperatures of the regenerated fibers were lower than that of the control fibers as the crystallinity changes. These changes were attributed to the thermal response of the regenerated cellulosic nanofibers. In view of the results from TGA, the induction of reformed cellulose crystal structures contributed to the thermal stability, suggesting that the nanocrystals partially broke the strong intermolecular hydrogen bonds of cellulose, as indicated in the XRD. It is well known that cellulose has a high thermal stability because of intermolecular hydrogen bonding. It is noted that a little decrease in the thermal stability of the materials would not influence its applicability as
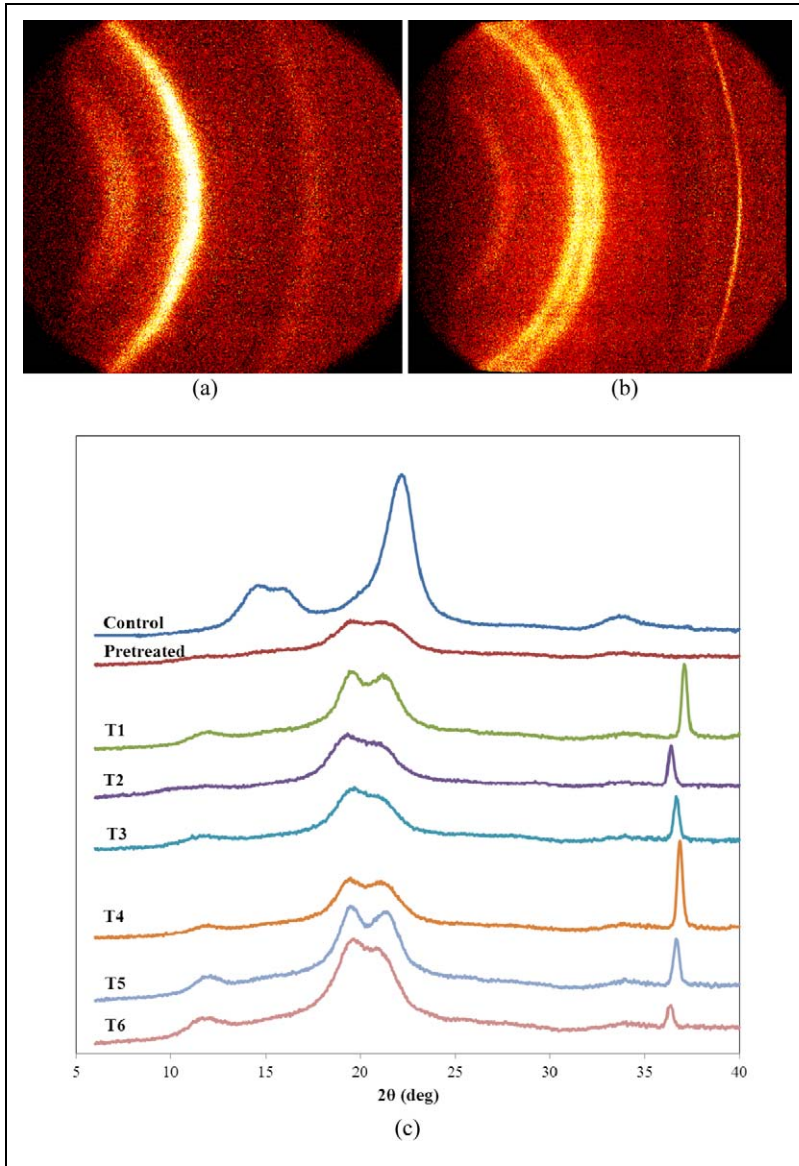
Figure 4. X-Ray diffraction patterns of native cellulose and regenerated cellulosic fibers from various treatment conditions. (a) Controlled fiber, (b) T6 regenerated nanofiber, and (c) all the fibers under different treatment conditions.

a reinforcement agent; however, changes in thermal stability could influence physical properties and mechanical performances of the nanocomposites incorporated with the crystallinity of the regenerated cellulose matrix in a variety of ways.

Table 2. Crystallinity and thermal characteristics of the regenerated cellulosic fibers coagulated from the aqueous gel.

	Crystallinity (%)	Thermal characteristics		
		T_{onset} (°C)	T_{peak} (°C)	T_{offset} (°C)
Control	63	291.5	307.7	321.4
Pretreatment	60	223.6	272.1	310.0
T1	53	208.4	251.9	299.5
T2	41	224.1	271.4	315.8
T3	41	267.6	296.2	316.5
T4	53	297.1	307.0	318.3
T5	53	287.0	302.6	315.5
T6	54	279.4	302.3	316.5

T_{onset}: onset temperature; T_{peak}: peak temperature; T_{offset}: offset temperature. T_1–T_6: treatment types.

Figure 5 shows the effect of treatment conditions on the surface morphology of congregated cellulose flakes and nanofibers. The control fibers showed the exposure of microfibers with extended surface openings to the aqueous solution. Pretreatment of the fibers with 17% NaOH provided the fiber with adequate swelling conditions to support chemical penetration and peeling off reaction at the microfibril interface. Cellulose nanofibers and their cross-linking are also clearly visible on the micrographs of the regenerated fiber samples. The smaller and denser pores were formed in the freeze-dried hydrogels. This suggests that the infused cellulose nanofibers were integrated to form a complex interwoven structure. Figure 5(c)-(e) show cellulose structures with flakes and the nanostructures dispersed in the cellulose matrix. High-magnified micrographs (Figure 5(f)-(h)) of the regenerated cellulose fibers showed the cellulose flakes with polysaccharide nanocrystal ball structures. Furthermore, the cross-linking condition would have played a significant role in the formation of the pore and crystal balls, especially in their size and shape.

Figure 6 illustrates the dependence of tensile strength on the 20% regenerated fiber reinforcement for the biocomposites. The reinforced polymer composites exhibit excellent mechanical properties, with values ranging from 28 to 34 MPa. In general, the addition of the cellulosic fillers regenerated from aqueous solutions without swelling agents resulted in decreased tensile strength. It is noted that the induction of inter-molecular interfaces with low crystallinity of the regenerated cellulose fibers decreased the mechanical properties of the polymer composites. The strength of nanocomposites reinforced with the regenerated fibers with swelling agents are nearly unchanged or slightly higher than the strength of the control fiber-reinforced samples. The regenerated nanocellulosic fibers formed a tight network to each fibers and the PP matrix locked the positions of the fibers. This may result in relatively strong strength properties of the composites, which can obtain the mechanical properties of the control fiber reinforcement.[22,23] This also implies that the nanofibers were incorporated into the PP matrix and
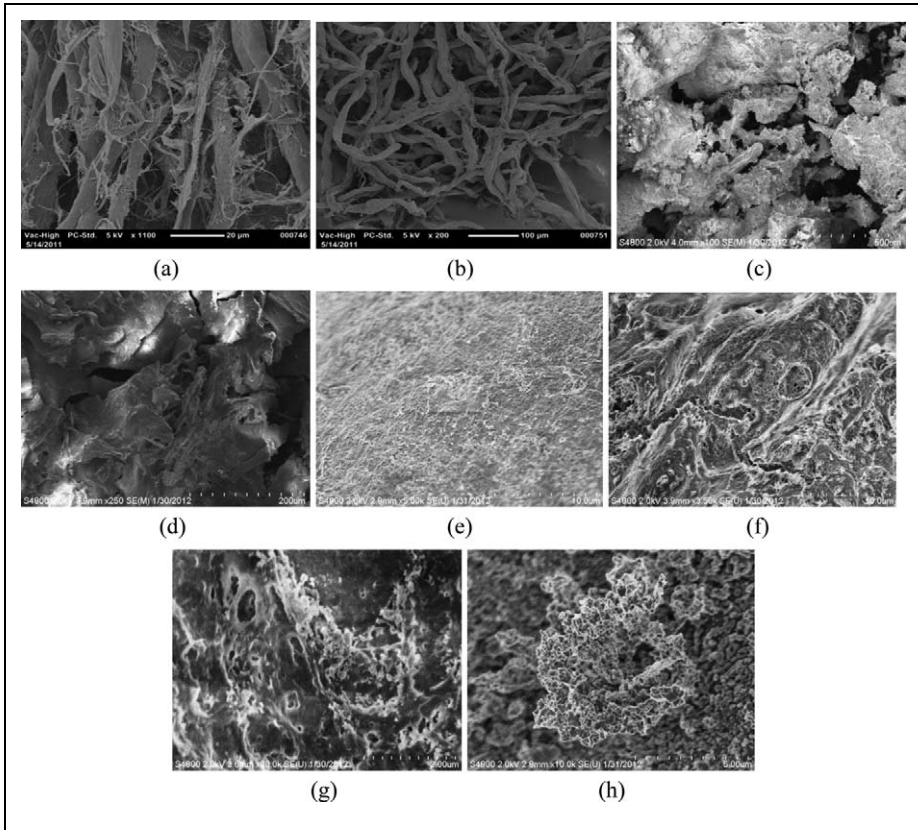
Figure 5. Surface morphology of the defiberated filter fibers and nanofibers generated from aqueous solutions. (a) Control, (b) pretreatment, (c) T4, (d) T5, (e) T6, (f) nanofiber web, (g) flakes, and (h) nanocrystal ball fibers coagulated with 5 wt% sulfuric acid.

established strong physical interactions between the PP matrix and regenerated nanocellulosic fibers.

Conclusions

This study described a simple process to obtain nanocellulosic fibers through the use of swelling agents in a cellulose/NaOH aqueous solution system. Cellulose was directly dissolved in the NaOH aqueous solution, with urea or thiourea as swelling agents to obtain a transparent solution. The H_2SO_4 and H_2O coagulants were successful in regenerating cellulosic fibers under ambient temperature. This study also found that lower treatment temperature provided better cellulose dissolution. Cellulose in the aqueous liquid gel formed regenerated nanocellulosic fibers without weight loss by the coagulation process. Urea and thiourea played an important role in the formation of
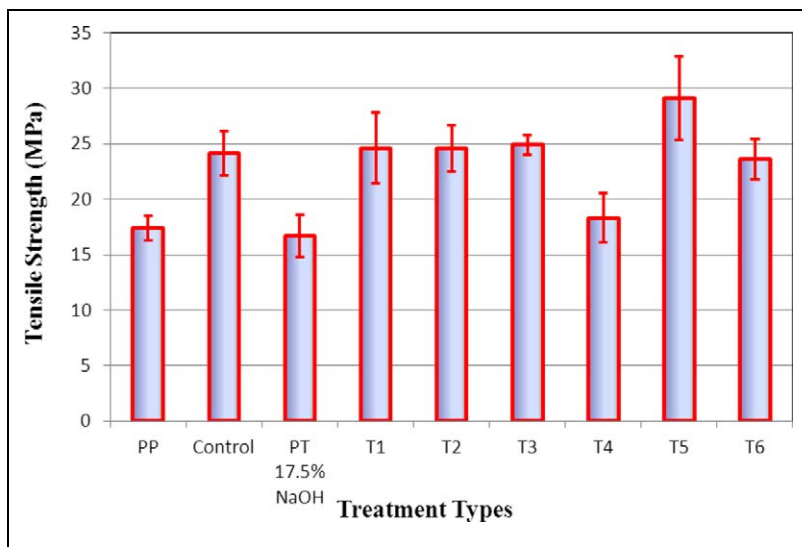
Figure 6. Tensile strength at break of the thin composite films compounded with 20% regener-ated nanocellulosic fibers and 80% PP as a matrix material.
PP: polypropylene; PT: pretreated.

cellulosic nanofibers. The results from WAXRD, FESEM, FTIR, TGA, and tensile testing confirmed crystal structure deformation, changed crystallinity, altered thermal characteristics, and effects on the mechanical performances of the regenerated nanocellulosic fibers. FESEM results indicated that the treatment broke the partial intermolecular hydrogen bonds of cellulose. The destructed and regenerated fibers possessed decreased crystallinity and resulted in the reduction of mechanical perfor-mance. However, the regenerated cellulosic fibers from cellulose/NaOH/urea and cellulose/NaOH/urea/thiourea aqueous solution systems provided better mechanical performance compared with those of reinforced fiber generated from cellulose/NaOH. The nanofibers in the composites acted as cross-links to create strong physical interac-tions to make up for the mechanical properties.

Funding

References

1. Isogai A and Atalla RH. Dissolution of cellulose in aqueous NaOH solutions. *Cellulose* 1998; 5: 309–319.
2. Jin H, Zha C and Gu L. Direct dissolution of cellulose in NaOH/thiourea/urea aqueous solution. *Carbohydr Res* 2007; 342(6): 851–858.
3. Zhang S, Li F, Yu J and Hsieh Y. Dissolution behaviour and solubility of cellulose in NaOH complex solution. *Carbohydr Polym* 2010; 81(3): 668–674.

4. Zhou J, Zhang L, Shu H and Chen F. Regenerated cellulose films from NaOH/urea aqueous solution by coagulating with sulfuric acid. *J Macromol Sci Physics B* 2002; 41(1): 1–15.

5. Egal M, Budtova T and Navard P. Structure of aqueous solutions of microcrystalline cellulose–sodium hydroxide below 0°C and the limit of cellulose dissolution. *Biomacromolecules* 2007; 8: 2282–2287.

6. Cai J, Wang L and Zhang L. Influence of coagulation temperature on pore size and properties of cellulose membranes prepared from NaOH–urea aqueous solution. *Cellulose* 2007; 14(3): 205–215.

7. Yang QL, Qi HS, Lue A, Hu K, Cheng GZ and Zhang LN. Role of sodium zincate on cellulose dissolution in NaOH/urea aqueous solution at low temperature. *Carbohydr Polym* 2011; 83(3): 1185–1191.

8. Atalla RH. Cellulose in carbohydrates and their derivatives including tannins, cellulose, and related lignins. In: *Comprehensive natural products chemistry*. Barton D. and Meth-Cohn O., Eds., Vol. 3. Oxford, UK: Elsevier Science Ltd, 1999, pp. 216.

9. Zhang S, Li F, Yu J and Gu L. Novel fibers prepared from cellulose in NaOH/thiourea/urea aqueous solution. *Fibers Polym* 2009; 10(1): 34–39.

10. Ke H, Zhou J and Zhang L. Structure and physical properties of methylcellulose synthesized in NaOH/urea solution. *Polym Bull* 2006; 56(4–5): 349–357.

11. Wang Y, Zhao Y and Deng Y. Effect of enzymatic treatment on cotton fiber dissolution in NaOH/urea solution at cold temperature. *Carbohydr Polym* 2008; 72(1): 178–184.

12. Qi H, Liebert T, Meister F and Heinze T. Homogeneous carboxymethylation of cellulose in the NaOH/urea aqueous solution. *Reactive Funct Polym* 2009; 69(10): 779–784.

13. Chen X, Burger C, Wan F, Zhang J, Rong L, Hsiao BS, et al. Structure study of cellulose fibers wet-spun from environmentally friendly NaOH/Urea aqueous solutions. *Biomacromolecules* 2007; 8(6): 1918–1926.

14. Fink HP, Weigel P, Purz HJ and Ganster J. Structure formation of regenerated cellulose materials from NMMO-solutions. *Prog Polym Sci* 2001; 26(9): 1473–1524.

15. Song Y, Zhou J, Zhang L and Wu X. Homogeneous modification of cellulose with acrylamide in NaOH/urea aqueous solutions. *Carbohydr Polym* 2008; 73(1): 18–25.

16. Ruan D, Huang Q and Zhang L. Structure and properties of CdS/regenerated cellulose nanocomposites. *Macromol Mater Eng* 2005; 290(10): 1017–1024.

17. Cai J, Zhang L, Zhou J, Qi H, Chen H, Kondo T, et al. Multifilament fibers based on dissolution of cellulose in NaOH/urea aqueous solution: structure and properties. *Adv Mater* 2007; 19(6): 821–825.

18. Walther A, Timonen J, Díez I, Laukkanen A and Ikkala O. Multifunctional high-performance biofibers based on wet-extrusion of renewable native cellulose nanofibrils. *Adv Mater* 2011; 23: 2924–2928.

19. Council of Europe. *Capillary viscometer method. European pharmacopoeia*. Vol. 1, 2.2.9. 5th ed. Strasbourg, France: European Directorate for the Quality of Medicines (EDQM), 2005, pp. 902.

20. Segal L, Creely JJ, Martin AE Jr, and Conrad CM. An empirical method for estimating the degree of crystallinity of native cellulose using the x-ray diffractometer. *Textile Res J* 1959; 29: 786–794.

21. American Society for Testing and Materials. *Standard test method for tensile properties of plastics*. Vol. 08.01. West Conshohocken, PA: ASTM D638-10. ASTM International, 2010.

22. Mukhopadhyay S, Deopura BL and Alagiruswamy R. Interface behavior in polypropylene composites. *J Thermoplast Compos Mater* 2003; 16(6): 479–495.

23. Lee S, Shupe TF, Groom LH and Hse CY. Maleated polypropylene film and wood fiber handsheet laminates. *Polymer Compos* 2009; 30(12): 1864–1872.